Biophysical Journal, Volume 96

Supplementary Material

Live Cell Linear Dichroism Imaging Reveals Extensive Membrane Ruffling Within the Docking Structure of Natural Killer Cell Immune Synapses

Richard K.P. Benninger, Bruno Vanherberghen, Stephen Young, Sabrina B. Taner, Fiona J. Culley, Tim Schnyder, Mark A.A. Neil, Daniel Wüstner, Paul M.W. French, Daniel M. Davis, and Björn Önfelt

Supplemental materials

Cell lines, chemicals and sample preparation

The B cell line 721.221 transfected to express MHC-HLA-Cw6 (221/Cw6) or GPI-GFP (221/GPI-GFP) and the NK-cell line YTS transfected to express KIR2DL1 have been described earlier (1, 2). The stable transfectants YTS/GPI-GFP, YTS/KIR2DL1/GPI-GFP, and YTS/YFP-Mem were generated by electroporation with linearized plasmids (GPI-GFP in pcDNA3.1, YFP-Mem, a kind gift from Gillian Griffiths, University of Cambridge (3)) and cultured under appropriate antibiotic selection. Stable transfectants expressing GPI-GFP or YFP-Mem were sorted for fluorescence by FACS (FACSDiva, Becton Dickinson). Cells were cultured in RPMI medium (Invitrogen, Carlsbad, CA) containing heat inactivated fetal bovine serum (FBS) (10%), L-glutamine (2mM) and penicillin-streptomycin (50 units/ml).

For imaging, 1-2×10^6 NK and target cells were washed separately in PBS or cell culture media and, for some of the experiments, stained with 3,3'dioctadecyloxacarbocyanine perchlorate (DiO) (Invitrogen, Carlsbad, CA) according to supplier's instructions. Thereafter NK and target cells were mixed and co-incubated for 30 minutes at 37 °C either in a cover slipped chamber (Nalge Nunc International, Rochester, NY) or a poc-chamber for live cell imaging, followed by imaging at 37 °C. For some of the confocal microscopy experiments cells (YTS/GPI-GFP) were fixed by incubation with 0.1% glutaraldehyde and 3.6% formaldehyde for 1 min at 37 °C followed by incubation with 3.6% formaldehyde for 5 min at room temperature.

Microscopy

Fluorescence images for protein distribution analysis were obtained using Leica DM IRE 2 (Leica Microsystems GmbH, Wetzlar, Germany) or Leica SP5 laser scanning confocal microscopes (LSCM) or a PerkinElmer UltraView (Weltham, MA, USA) spinning disc confocal microscope. For LSCM, the image settings were defined empirically to maximize the signal:noise ratio and to avoid saturation. Series of bright-field and confocal fluorescence images were simultaneously obtained. The distributions of fluorescent probes were tracked by z-stack acquisition (30-90 individual planes 0.3-0.6μm apart). For time-lapse imaging confocal stacks were acquired at 30-second to 2-minute intervals for time periods ranging from 10 minutes to 2 hours.

The laser setup used for LD imaging has previously been described in detail (4). Briefly, illumination is provided by a mode-locked Ti:Sapphire laser (Tsunami, Spectra Physics, Mountain View, CA) that produces pulses with ~100 fs full-width at half maximum (FWHM), at a repetition rate of 80 MHz and with an average power of ~1.2 W at 920 nm. The optical set-up is

a commercially available multi-focal (up to 64 separate foci) multiphoton microscope (TriMScope, LaVisionBiotec GmbH, Bielefeld, Germany) connected to a modified inverted microscope (IX-71, Olympus corporation, Tokyo, Japan) in epi-illumination geometry. On the imaging side, a polarization resolved imager (Optical Insights, Santa Fe, NM) splits the image of the sample into 2 sub-images of orthogonal polarizations using a polarizing beam splitter, one polarized parallel to the incident illumination, the other perpendicular. These two sub-images are incident onto a cooled, front illumination electron multiplying CCD (Ixon, Andor Technology, Belfast, N. Ireland). Imspector software developed by LAVisionBiotec was used to control all of the instrumentation.

For 2D LD imaging the focus was adjusted such that the two-photon excitation was at the midsection of the cell. Several frames were acquired with the EMCCD at high gain and averaged. Since horizontal and vertically polarized emissions are simultaneously imaged on the CCD chip, these two separate sub-images need to be spatially overlapped before forming the LD. This is performed using home developed routines in LabView (National Instruments, Austin, TX) where the two images are translated, stretched and rotated, such that every part of the cell overlaps spatially within an error of one pixel. Thus we have images of I_{ZZ}, I_{ZY}, I_{YZ} and I_{YY}. The G factor is measured to correct for the fact that the imaging side of the set-up could preferentially transmit one particular polarization over the other. Similarly, the excitation intensity could be greater at one polarization than the other, and, therefore, also an excitation factor (E) is employed to correct for this. The G and E factors are calculated by imaging a homogenous solution of fluorescein with the same scan settings as for the excitation of the cell. The LD^r image is formed as follows from the cell images, G and E factors:

$$LD^r = \frac{\left(I_{ZZ} + 2GI_{ZY}\right) - E\left(I_{YY} + 2G^{-1}I_{YZ}\right)}{\left(I_{ZZ} + 2GI_{ZY}\right) + 2E\left(I_{YY} + 2G^{-1}I_{YZ}\right)} \qquad (1)$$

These images are generated with home developed routines in MATLAB (Mathworks, Natick, MA) and are represented as HSV images, where Hue encodes the LD^r value, and Value encodes the calculated isotropic absorption or emission intensity, and Saturation is at a constant maximum.

Image analysis

Quantification of fluorescence distribution in the plasma membrane was performed using the software ImageJ (National Institute of Mental Health, Bethesda, Maryland, USA) by defining three different regions of the plasma membrane; 1) the center of the IS, 2) the periphery of the IS

and 3) outside the IS. The average fluorescence intensity, only selecting pixels with an intensity value above a threshold corresponding to the background noise, was determined for each region, and normalized to the average value found in the plasma membrane outside the IS for each cell. The software Volocity (Improvision, Coventry, England) was used to visualize 3D projections of cell images.

For quantitative analysis of the membrane ruffling, the LD^r was determined as a function of the angle between the plasma membrane and excitation polarization, for the three different regions of the plasma membrane (center, periphery and outside of the IS). For each cell, the LD^r was averaged over one or more small areas (~1μm^2) in each region of the plasma membrane, using home developed routines in LabView. A tangent is drawn to the plasma membrane at each of these areas, and the angle between the tangent and the excitation polarization is calculated, as is depicted in Figure 2 A (main text) by the angle θ. This experimental data can then be fitted to a model of the variation of LD^r with plasma membrane angle θ. This model is described in detail in (4) (note the different notion where θ is described as α), and is summarized below.

Briefly, for a given plasma membrane angle (θ), microscopic fluorophore orientation (φ) and sub-resolution membrane ruffling (η) (Figure S1), the absorption of single DiO fluorophores following vertically and horizontally polarized excitation can be calculated ($A_{||,\perp}(\theta,\varphi,\eta)$).

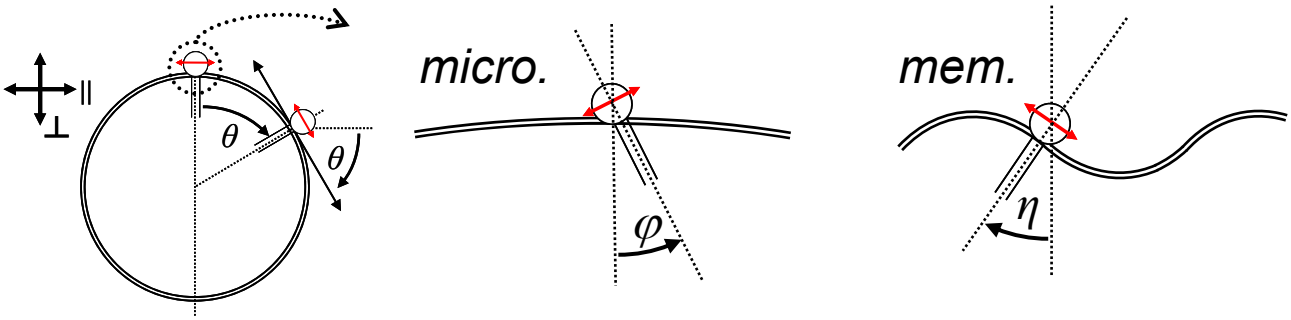

Figure S1. Schematic of the orientation angles considered for the DiO fluorophore (red arrow indicates the dipole moment) when calculating the LD^r. Left: the angle the plasma membrane makes with the parallel excitation axis is labeled θ. Middle: The orientation of the DiO fluorophore defined by molecular interactions with membrane lipids is labeled as φ. Right: The orientation of the DiO fluorophore defined by membrane topology is labeled as η (in this panel $\varphi = 0$).

By integrating the absorption from a single molecule over all populated microscopic fluorophore orientations (*micro.*) and all membrane ruffling orientations (*mem.*), the total absorption from an ensemble of DiO fluorophores at plasma membrane angle θ can be calculated:

$$\left\langle A_{||,\perp}(\theta)\right\rangle = \int_{mem.} d\eta \int_{micro.} d\varphi \cdot A(\theta,\varphi,\eta) \qquad (2)$$

Thus the variation in LD^r with plasma membrane angle can be calculated for a given microscopic DiO fluorophore orientation and membrane ruffling:

$$LD^r(\theta) = \frac{\langle A_{\parallel}(\theta)\rangle - \langle A_{\perp}(\theta)\rangle}{\langle A_{\parallel}(\theta)\rangle + 2\langle A_{\perp}(\theta)\rangle} \quad (3)$$

Qualitatively, if there is a random (isotropic) DiO orientation there will be no variation of LD^r with θ. Conversely, if there is a high degree of DiO orientation there will be a large variation of LD^r with θ. We have previously shown that the LD^r of DiO is largely unaffected by cholesterol depletion from the cell membrane, showing that the microscopic orientation of DiO is insensitive to the membrane composition (4). Therefore the variation in LD^r of DiO with θ is a relative measurement of the degree of sub-resolution membrane ruffling in this localized region of the cell. Thus, no variation of LD^r with θ indicates extensive membrane ruffling, whereas a large variation of LD^r with θ indicates little membrane ruffling.

Quantifying relative degree of membrane ruffling

From the variation of LD^r with plasma membrane angle θ, we can quantify the relative degree of membrane ruffling that occurs at the synapse compared to the plasma membrane outside the synapse. A functional form of the membrane ruffling topology must be assumed. We choose to describe the cross section of the membrane Y(x) in terms of a sinusoid:

$$Y(x) = H\sin(x) \quad (4)$$

Where H describes the modulation depth of the membrane ruffling (Figure S2).

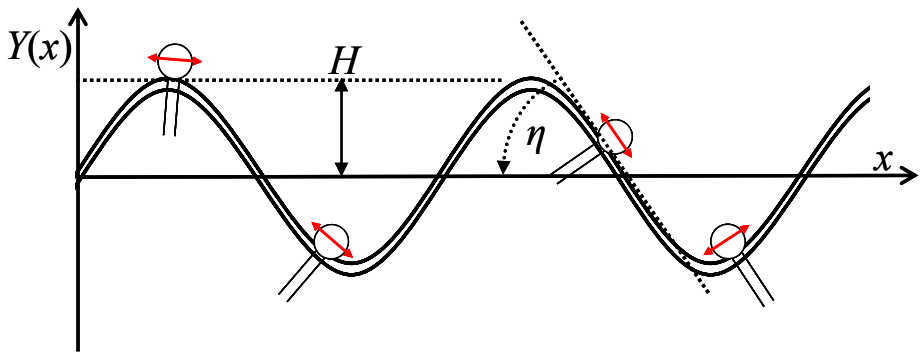

Figure S2. Schematic of sinusoidal plasma membrane ruffling $Y(x)$, where H is the depth of modulation, and η is the angle representing the deviation of the membrane normal due to ruffling.

At a point along the membrane x, the angle that the membrane ruffle forms (η) can be calculated:

$$\eta \approx \tan^{-1}\left(\frac{dY(x)}{dx}\right) = \tan^{-1}\left(H\cos(x)\right) \qquad (5)$$

Thus the ensemble averaged absorption ($A_{||}(\theta)$, $A_{\perp}(\theta)$), averaged over all membrane ruffling (corresponding to the integral *mem.* in equation 2) along the membrane of length X is:

$$\left\langle A_{\parallel,\perp}(\theta)\right\rangle \approx \int_0^X A_{\parallel,\perp}\left(\theta,\eta = \tan^{-1}\left\{H\cos(x)\right\}\right)dx \qquad (6)$$

This is evaluated numerically, and the resultant LD^r is calculated according to equation 3.

We will assume that outside the docking structure, the plasma membrane is flat such that the relative membrane ruffling induced at the periphery and center of the docking structure are calculated. For a membrane orientation θ=0, the mean microscopic DiO orientation (φ) is calculated according to equation 2 for the experimental LD^r measured outside the synapse (0.279±0.036). We then calculate, using equations 5 and 6, the modulation in membrane topology (H) that is required to give the LD^r measured at the centre of the synapse (0.254±0.031) and the periphery of the synapse (0.035±0.015). The calculated H - values were 1.38 for the periphery and 0.24 for the center of the docking-structure, respectively. A graphical representation of the relative degree of membrane ruffling is shown in the main text (Figure 3C).

Effect of intracellular vesicles on LD^r

As discussed in the main text, the accumulation of lipid vesicles at the plasma membrane of the immune synapse could account for a decrease in the LD^r signal, since the integrated DiO orientation in each vesicle will be zero. We show here the calculation that determines the net LD^r signal that would be measured depending on the concentration of vesicles that occurs at the plasma membrane.

The net LD^r ($LD^r_{net(\theta)}$) is the average of the LD^r of DiO in the plasma membrane and the vesicles (LD^r_{PM}, $LD^r_{ves.}$ respectively):, weighted by isotropic absorption (A_{PM}, $A_{ves.}$ respectively):

$$LD^r_{net}(\theta) = \frac{\left(A_{PM}LD^r_{PM}(\theta) + A_{ves.}LD^r_{ves.}(\theta)\right)}{\left(A_{PM} + A_{ves.}\right)} \qquad (7)$$

The LD^r of the plasma membrane has already been experimentally measured with $LD^r_{PM}(0)$ being 0.279±0.037 (blue curve in Figure 3 A of the main text). The LD^r of sub-resolution lipid vesicles will be zero for all θ, $LD^r_{ves}(\theta) = 0$:

$$LD^{r}{}_{net}(\theta) = \frac{A_{PM}}{A_{PM} + A_{ves.}} LD^{r}{}_{PM}(\theta) \qquad (8)$$

Thus, the decrease in LD^r at the synapse periphery compared to the plasma membrane outside the synapse is a function of the relative amount of membrane from vesicles compared to plasma membrane (Figure S3). The net LD^r that is experimentally measured at the synapse periphery is shown by the black curve in figure 3 A of the main text, with $LD^{r}{}_{net}(0)$ being 0.035±0.015. For this reduction in LD^r to be due to lipid vesicles stacked underneath the plasma membrane surface, the relative absorption of DiO in the vesicles would be:

$$\frac{A_{PM} + A_{ves.}}{A_{PM}} = \frac{LD^{r}{}_{PM}(\theta)}{LD^{r}{}_{net}(\theta)} = \frac{0.279}{0.035} = 7.97 \longrightarrow A_{ves.} \approx 7A_{PM} \qquad (9)$$

Thus if we consider per unit area of plasma membrane that DiO in a saturated layer of lipid vesicles would have ~3 times (π times- see figure S3) the isotropic absorption of DiO in the plasma membrane, there would have to be >2 saturated layers of vesicles to result in the reduction in LD^r that we measure at the periphery of the immune synapse.

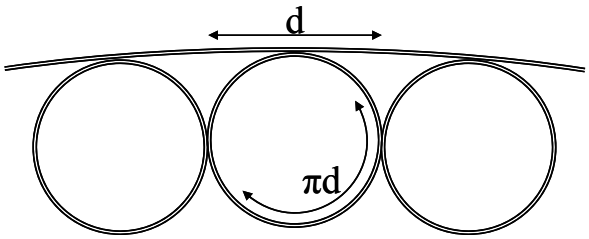

Figure S3. Schematic showing lipid vesicles in contact with the plasma membrane. When the vesicles are closely packed, the amount of lipid material in the vesicles per unit area of plasma membrane is π (~3.14) times that of the plasma membrane. The isotropic absorption due to one layer of vesicles will therefore be ~3 times more than that due to a flat plasma membrane

Since neither of the two vesicle-associated proteins, lysosomal-associated membrane protein 1 (LAMP1) and transferrin receptor (TfR), showed increased intensity to the periphery (data not shown), we can conclude that it is highly unlikely the loss in LD^r is due to the presence of lipid vesicles stacked underneath the plasma membrane.

References

1. Davis, D. M., I. Chiu, M. Fassett, G. B. Cohen, O. Mandelboim, and J. L. Strominger. 1999. The human natural killer cell immune synapse. *Proc Natl Acad Sci U S A* 96:15062-15067.
2. Önfelt, B., S. Nedvetzki, K. Yanagi, and D. M. Davis. 2004. Cutting edge: Membrane nanotubes connect immune cells. *J Immunol* 173:1511-1513.

3. Stinchcombe, J. C., G. Bossi, S. Booth, and G. M. Griffiths. 2001. The immunological synapse of CTL contains a secretory domain and membrane bridges. *Immunity* 15:751-761.
4. Benninger, R. K. P., B. Önfelt, M. A. A. Neil, D. M. Davis, and P. M. W. French. 2005. Fluorescence Imaging of Two-Photon Linear Dichroism: Cholesterol Depletion Disrupts Molecular Orientation in Cell Membranes. *Biophys. J.* 88:609-622.